Corrosion Science 51 (2009) 1441–1452

Contents lists available at ScienceDirect

Corrosion Science

journal homepage: www.elsevier.com/locate/corsci

Self-assembled monolayer of 2-(octadecylthio)benzothiazole for corrosion protection of copper

B.V. Appa Rao [a,*], Md. Yakub Iqbal [a], B. Sreedhar [b]

[a] Department of Chemistry, National Institute of Technology, Warangal 506004, Andhra Pradesh, India
[b] Inorganic & Physical Chemistry Division, Indian Institute of Chemical Technology, Hyderabad 500007, India

ARTICLE INFO

Article history:
Received 8 August 2008
Accepted 25 March 2009
Available online 2 April 2009

Keywords:
A. Copper
B. EIS
B. Polarization
B. XPS

ABSTRACT

Self-assembled monolayer (SAM) of 2-(octadecylthio)benzothiazole (2-OTBT) was formed on a fresh copper surface obtained by nitric acid etching. Optimum conditions for formation of SAM have been established. XPS, AFM and FTIR studies have been used to characterize the SAM. Corrosion protection ability of the SAM has been evaluated in aqueous NaCl solution using electrochemical impedance, EQCN, potentiodynamic polarization and weight-loss studies. 2-OTBT SAM is found to have excellent corrosion protection efficiency in the aq. NaCl solution. The mechanism of corrosion inhibition of copper by 2-OTBT SAM is discussed.

1. Introduction

Copper is an important metal which is used in creating multilevel interconnecting structures in the ultra large scale integrated circuits, due to its high electrical conductivity and resistance to electro migration [1,2]. Prevention of copper oxidation in copper metallization technology is one of the major challenges. Copper is also widely used in electronic packaging, such as copper lead frames, interconnection wires, foils for flexible circuits, heat sinks etc. Copper lead frame serves mainly to support the chip mechanically during the assembly of plastic package and to connect the chip electrically with the outside world. Copper foil is the most commonly used conductor for flexible circuits and flexible interconnections. Heat sink is used to transport heat dissipated by devices to a heat exchanger or to spread it over a large surface area to facilitate cooling by radiation or convection. At present the most widely used heat sink is the laminated metal sandwich consisting of two layers of copper bonded to a central constraining layer of molybdenum. Corrosion of copper is considered a serious reliability problem in microelectronic packaging. The primary effects of corrosion of copper in interconnection wires and copper lead frames are as follows. Corrosion of copper at the interface of Cu–Al bonding area causes decrease in the interfacial shear strength and weakens the Cu–Al bonding [3]. Corrosion of copper in the area of the copper lead frames die pad and molding compound causes the delamination of packages. Initial corrosion of copper induces poor adhesion in the area of copper lead frames and molding compound, so that moisture is able to penetrate through the crevices, aggravating the corrosion problem in packages further. Self-assembled monolayers (SAMs) are dense and ordered monolayers [4], which act as effective barriers and protect copper against corrosion. Laibinis and Whitesides reported that alkanethiols adsorbed on copper surface form densely packed SAMs, which were found to be effective inhibitors of copper corrosion in air [5]. Feng et al. reported the corrosion protection of self-assembled alkanethiol monolayer on copper in a 0.5 M NaCl solution [6]. Aramaki reported that the maximum efficiency of the SAM of octadecanethiol for protection of corrosion of copper in 0.5 M Na_2SO_4 solution was 80.3% [7]. Quan et al. studied the corrosion protection ability of the SAMs of schiff bases on copper surfaces [8,9]. Every and Riggs found that the corrosion inhibition efficiency of sulfur containing compounds is generally superior to that of nitrogen containing compounds [10]. However, no studies have been reported in the literature on SAMs on copper surface using heterocyclic compounds with long alkyl chains. 2-(octadecylthio)benzothiazole (2-OTBT) is a heterocyclic long alkyl chain organic compound containing one nitrogen atom and two sulfur atoms. It was of interest to investigate into the corrosion protection efficiency of 2-OTBT SAM on copper surface and the mechanistic aspects of corrosion inhibition. The structure of 2-OTBT used for the formation of SAM as per ChemDraw Ultra 8.0 version is shown in Fig. 1.

* Corresponding author. Tel.: +91 870 2462652; fax: +91 870 2459547.
E-mail addresses: boyapativapparao@rediffmail.com, chemysri@yahoo.com (B.V. Appa Rao), yakub_iqbal@yahoo.com (Md. Yakub Iqbal).

0010-938X/$ - see front matter © 2009 Elsevier Ltd. All rights reserved.
doi:10.1016/j.corsci.2009.03.034

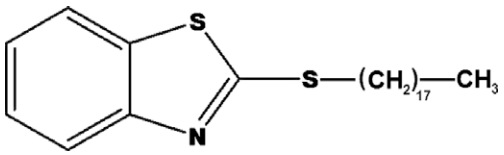

Fig. 1. Structure of 2-(octadecylthio)benzothiazole.

2. Experimental

2.1. Materials and solutions

2-OTBT was synthesized by mixing equimolar amounts of 1-bromo octadecane and benzothiazole-2-thiol in round-bottomed flask in the presence of a solvent mixture of *N*,*N*-dimethylformamide and anhydrous ethanol and then refluxing for 6 h [11]. Differential scanning calorimetry and ^{1}H NMR spectroscopy were used for characterization of 2-OTBT. Purity of 2-OTBT was assessed by high performance liquid chromatography. It was found that the 2-OTBT was 99.0% pure. Eight hundred and thirty-eight milligram of 2-OTBT was dissolved in ethyl acetate solvent to get a 20 mM solution. 5 mM, 10 mM and 15 mM solutions were prepared from the 20 mM solution by dilution. For weight-loss studies, the copper specimens of the dimensions $4 \times 1.0 \times 0.2$ cm were used, while for other studies, the dimensions of the specimens were $1.0 \times 1.0 \times 0.2$ cm. These specimens were polished to mirror finish using 1/0, 2/0, 3/0, 4/0 grade emery papers and alumina powder on rotating disk and then degreased with acetone. The specimens were washed with double distilled water and dried.

2.2. Formation of self-assembled monolayers

Solubility of 2-OTBT was tested in the organic solvents such as ethanol, methanol, acetone, chloroform, ethyl acetate and *n*-hexane. It was found that 2-OTBT is insoluble in other solvents except ethyl acetate and *n*-hexane and the solubility in ethyl acetate is relatively less than that in *n*-hexane. Both ethyl acetate and *n*-hexane were chosen as solvents for formation of 2-OTBT SAM on copper surface. The polished copper specimens were etched with 7 N nitric acid for 30 s, washed with triple distilled water followed by the organic solvent as quickly as possible and then immediately immersed in different concentrations of 2-OTBT solution in organic solvent for various immersion periods.

2.3. Electrochemical impedance and polarization studies

Electrochemical impedance studies were first carried out in order to establish the optimum conditions for the formation of protective SAM on copper surface. The impedance studies were carried out in a three-electrode cell assembly (in accordance with ASTM specifications) using an electrochemical workstation model IM6e ZAHNER elektrik, Germany. The bare copper specimen or the 2-OTBT SAM modified copper specimen was used as the working electrode. A platinum electrode was used as the counter electrode and the reference electrode was a silver–silver chloride electrode. Impedance measurements were carried out at the open-circuit potential in the frequency range from 60 kHz to 10 mHz and Nyquist plots were obtained. The impedance studies were also carried out in order to investigate the corrosion protection ability of the SAM in an aggressive environment viz., NaCl in the concentration range of 0.02–0.20 M, at various immersion periods (0.5–24 h) and at various temperatures (30–60 °C). Inhibition efficiencies were calculated from the impedance data. Potentiodynamic polarization studies were carried out in a three-electrode cell assembly at different concentrations (0.02–0.20 M) in NaCl environment using the same electrochemical workstation and the cell assembly used for impedance studies. The polarization curves were recorded in the potential range of −0.500 V to +0.200 V vs. Ag/AgCl at a scan rate of 1 mV/s. Correction of the curves for IR-drop compensation was not required because of the high electrical conductivity of the aggressive corrosive environments [12]. The reference electrode was kept very near to the working electrode.

2.4. Studies using electrochemical quartz crystal nanobalance

Electrochemical quartz crystal nanobalance system, model Elchema EQCN-700 and an AT-cut copper quartz crystal with 10 MHz nominal frequency were used in these studies. The copper quartz crystal was immersed in the 2-OTBT solution in ethyl acetate solvent and the mass change as a function of time up to 24 h was recorded during the formation of SAM on the copper crystal. The corrosion protection ability of the 2-OTBT SAM was also found using EQCN studies. The 2-OTBT modified copper quartz crystal was immersed in 0.02 M NaCl solution and the mass change was recorded as a function of time up to 24 h. A positive mass change indicates mass gain and a negative mass change indicates mass loss.

2.5. Contact angle measurements

Contact angle measurements for bare copper and copper covered with 2-OTBT SAM were made by sessile water drop method using a contact angle measuring system, model G10, Kruss, Germany. The measurements were carried out at about 30 °C in air.

2.6. Surface analysis by Fourier transform infrared (FTIR) spectroscopy

FTIR measurements for bare copper and copper covered with SAM were recorded in single reflection mode using FTIR spectrophotometer, model Nexus 670 of the Thermo Electron Corporation, USA in the spectral range of 400–4000 cm^{-1} with a resolution of 4 cm^{-1}. Bare copper and 2-OTBT SAM covered copper specimens were mounted on the reflection accessory and the plane polarized light was incident at a grazing angle of 85° from the surface normal. The sample compartment was continuously purged with nitrogen during the measurement.

2.7. Surface analysis by AFM

The AFM senses repulsive contact forces between a fixed flexible micro cantilever and the surface of the sample. The Z motion of a silicon nitride tip was monitored in height mode by mounting the sample on an X-Y-Z piezoelectric tube scanner. Veeco Nanoscope IV multimode AFM was used for studying the morphology of copper surface covered with SAM. AFM studies were also used to observe changes in the morphology of the SAM covered copper surface in the presence of a corrosive environment, namely 0.02 M NaCl.

2.8. Surface analysis by X-ray photoelectron spectroscopy (XPS)

The surface analysis of bare copper and 2-OTBT SAM covered copper was carried out using the X-ray photoelectron spectrometer, ESCA Kratos model AXIS-165, with Mg Kα radiation (1253.6 eV) and sensitivity of 0.1 eV. Computer deconvolution was applied to detect the elemental peaks of copper, oxygen, carbon, nitrogen and sulfur present in the SAM. XPS studies were also used to analyze the nature of the surface films in the presence of a corrosive environment, 0.02 M NaCl.

2.9. Weight-loss studies

The bare copper specimens and the copper specimens covered with SAM were immersed in 0.02 M NaCl solution for a period of 3 days. The weights of the specimens before and after immersion were recorded by using an electronic balance with a readability of 0.01 mg. From the weight-loss data, the corrosion rates and inhibition efficiencies were calculated.

2.10. Quantum chemical calculations

Quantum chemical calculations were carried out using semi-empirical AM1 molecular orbital method in the MOPAC program using Chem3D Ultra Molecular Modelling and Analysis software 8.0 version. E_{HOMO}, E_{LUMO}, ΔE, net atomic charges on each of the elements of 2-OTBT and the total ring charge were obtained from these calculations.

3. Results and discussion

3.1. Optimum conditions for formation of 2-OTBT SAM

The formation process of the self-assembled monolayer can be classified into two steps, namely fast adsorption as the first step and then a slow rearrangement, as described by Rondelez et al. [13] and it is shown in Fig. 2. With increase in immersion time, the film becomes denser and more stable. To obtain a dense and stable SAM, the best immersion time was reported to be more than 20 h by Quan et al. [8] in their studies on formation of SAM of schiff base on copper and a concentration of 5 mM was reported to be the optimum concentration [14]. Therefore, in the present study an immersion period of 24 h and 5 mM concentration of 2-OTBT were fixed initially for the study of formation of SAM in the solvents namely ethyl acetate and *n*-hexane. Nyquist plots were recorded separately for the SAM covered copper electrodes in both the solvents. Nyquist plot of the SAM formed from the solution in ethyl acetate showed no Warburg impedance and yielded much higher charge transfer resistance. Therefore, ethyl acetate was finally chosen as the solvent. The effect of surface treatment of the copper specimen on the quality of 2-OTBT SAM was investigated by comparing the impedance parameters of copper covered with SAM formed after etching the copper surface in 7 N nitric acid and without etching. In this study the immersion period as 24 h, the concentration of 2-OTBT as 5 mM and ethyl acetate as solvent were chosen. It was found from the Nyquist plots that the nitric acid etching of copper surface is necessary for formation of a protective 2-OTBT SAM. The effect of concentration of 2-OTBT on the quality of SAM is shown in Fig. 3A. It is evident from these results that the R_{ct} value is much higher and the Warburg impedance also disappeared in the case of SAM formed from 20 mM concentration of 2-OTBT, when compared with lower concentrations. Therefore 20 mM was chosen as the optimum concentration for formation of dense and protective SAM. By fixing the concentration of the 2-OTBT solution as 20 mM, Nyquist plots were obtained at different immersion periods in the range of 3–24 h in 300 ppm chloride environment and are shown in Fig. 3B. The SAM formed after 24 h has the highest R_{ct} value. Hence an immersion time of 24 h was chosen in the studies.

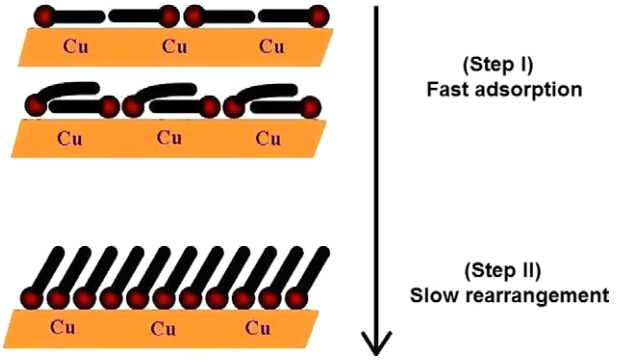

Fig. 2. Schematic diagram of formation of SAM.

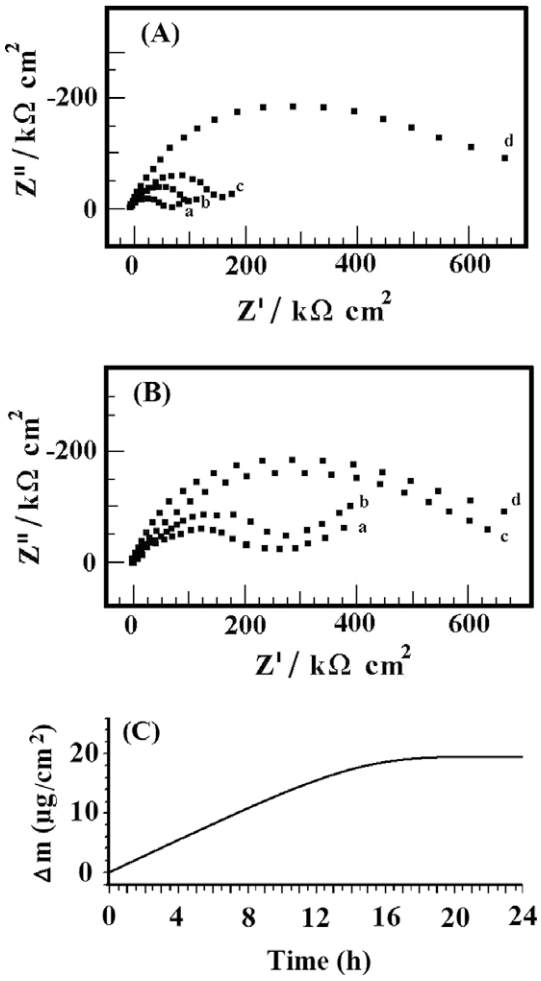

Fig. 3. (A) Nyquist plots of copper with SAM formed at constant immersion period of 24 h and at different concentrations of 2-OTBT. a – 1 mM, b – 5 mM, c – 10 mM, d – 20 mM (Environment: aq. 300 ppm chloride). (B) Nyquist plots of copper with SAM formed in 20 mM 2-OTBT at different immersion periods. a – 3 h, b – 6 h, c – 12 h, d – 24 h (Environment: aq. 300 ppm chloride). (C) Mass change vs. time curve during formation of SAM on copper quartz crystal in the presence of 2-OTBT in ethyl acetate.

Electrochemical quartz crystal nanobalance (EQCN) is capable of detecting mass changes in the nanoscale range. Several investigations were carried out to investigate the copper electrode behavior in corrosive environments using EQCN [15–20]. The oscillation frequency of a quartz crystal is highly sensitive to the minute mass changes at the crystal surface. One face of the crystal is modified to function as the working electrode and changes of the electrode mass were continuously monitored [21,22]. Fig. 3C shows the mass change vs. time plot obtained from EQCN experiment. The curve represents the change of mass on the copper quartz crystal surface as a function of time when immersed in a 20 mM solution of 2-OTBT in ethyl acetate. The increase of mass is due to the formation of monolayer of 2-OTBT on the copper surface. A positive mass change is observed up to 19 h and thereafter, the change in mass

is negligible. It can therefore be concluded that the minimum time required for complete formation of 2-OTBT SAM on copper surface is 19 h.

Based on all the above results, it can be inferred that the optimum conditions for the formation of 2-OTBT SAM on copper surface are (i) etching of copper surface in 7 N nitric acid for 30 s (ii) ethyl acetate solvent (iii) 20 mM concentration of 2-OTBT and (iv) immersion time of 24 h. These conditions were used for formation of 2-OTBT SAM on copper throughout the studies.

3.2. Characterization of 2-OTBT SAM

3.2.1. Contact angle measurements

The degree of hydrophobicity of 2-OTBT SAM is characterized by the contact angle measurement of a sessile water drop on the copper surface covered with SAM. The contact angle values for bare copper and SAM covered copper are found to be 78° and 91° respectively. The contact angle value for the 2-OTBT SAM covered copper surface indicates the hydrophobic nature of the self-assembled monolayer, which in turn provides a barrier against corrosive species from attacking the underlying copper substrate. It is worth mentioning that the contact angle values reported in the literature for the SAMs of hexadecane thiol [23], octadecanoyl hydroxamic acid [24], benzene thiol and 4-amino benzene thiol [25] on copper surface are 120°, 108°, 100° and 95° respectively. From these values it can be inferred that the degree of hydrophobicity is higher in the case of SAMs formed by the aliphatic organic molecules having long alkyl chain. The degree of hydrophobicity of 2-OTBT SAM is comparable to that of the SAM formed by 4-amino benzene thiol.

3.2.2. X-ray photoelectron spectroscopic studies

In the XPS spectrum of bare copper, Cu $2p_{3/2}$, Cu $2p_{1/2}$ and O 1s peaks are detected. The computer deconvolution XPS spectra for copper and oxygen are shown in the Fig. 4A and B respectively. The Cu $2p_{3/2}$ peak at a binding energy of 932.6 eV and the Cu $2p_{1/2}$ peak at 952.4 eV can be attributed to Cu (I) [4]. The O 1s peak observed at 531.1 eV is therefore due to formation of Cu_2O on the copper surface [26,27], which is formed during the interval between polishing of the copper surface and the XPS analysis.

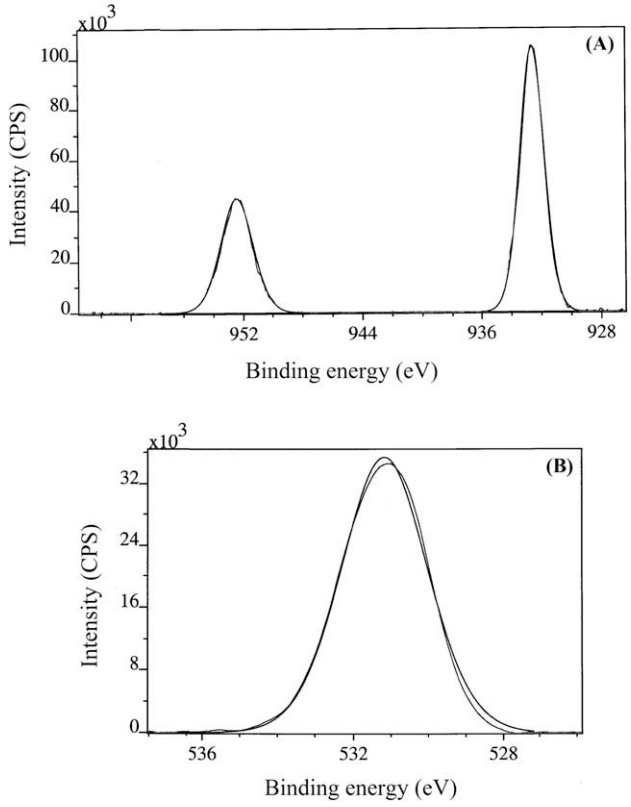

Fig. 4. (A and B) XPS deconvolution spectra of different elements present on the surface of the bare copper (4A – Cu 2p, 4B – O 1s).

The XPS spectrum of copper surface modified with 2-OTBT SAM shows peaks corresponding to Cu $2p_{3/2}$, Cu $2p_{1/2}$, O 1s, C 1s, N 1s and S 2p. The computer deconvolution spectra for copper, oxygen, carbon, nitrogen and sulfur are shown in the Fig. 5A–E, respectively. The peaks at 932.2 eV for Cu $2p_{3/2}$ and 952.2 eV for Cu $2p_{1/2}$ can be attributed to Cu (I), which is due to initial oxidation of copper surface to Cu_2O during SAM formation [28]. Kamdem et al. reported in their studies that the Cu $2p_{3/2}$ peak at 935 eV and the presence of shake up satellites indicate the presence of cupric copper, while the peak around 933 eV and the absence of shake-up satellites indicate the presence of cuprous copper [29]. Therefore it can be inferred that the peak observed in our studies at 932.2 eV without any shake-up satellites is due to the presence of cuprous copper in the 2-OTBT SAM modified copper. The O 1s peak observed at 531.6 eV, is due to formation of Cu_2O on the copper surface during SAM formation. The existence of oxygen in the SAM shows that the oxygen dissolved in the solution has taken part in the self-assembly process, by oxidizing the copper surface to Cu_2O [4]. C 1s shows peaks at 284.5, 286.1 and 288.5 eV respectively. The intense C 1s peak at 284.5 eV arises due to the presence of 18 carbon atoms in the alkyl chain of 2-OTBT [30]. The C 1s peaks at 286.1 and 288.5 eV are due to two different carbon environments present in the aromatic ring of 2-OTBT. The N 1s peak is observed at 398.7 eV, while the characteristic binding energy of the elemental nitrogen is reported as 398.0 eV in the literature [31]. The shift of N 1s binding energy from elemental binding energy indicates that nitrogen plays a vital role in complex formation between copper and 2-OTBT SAM. Fig. 5E shows the S 2p peaks of the 2-OTBT modified copper substrate. The two peaks at 163.7 and 165.0 eV are due to S $2p_{3/2}$ and S $2p_{1/2}$ components. There is a theoretical separation of 1.3 eV between the two peaks. These peaks are attributable to the sulphur with a lone pair of electrons present in the ring as well as in the form of substituent. It may be noted that the chemical environment of both the sulphur atoms in the molecule is similar. In the literature when SAM formation was done through a thiolate group namely RS^-, the two peaks due to S $2p_{3/2}$ and S $2p_{1/2}$ were reported at 162.5 and 163.7 eV respectively [5,25]. It must be noted that in the present study in the case of 2-OTBT SAM sulphur is not present as thiolate but as sulphur with a lone pair of electrons and hence the observed slightly higher binding energy values of the two S 2p peaks.

3.2.3. FTIR reflection absorption studies

FTIR reflection absorption spectra for bare copper and the copper covered with 2-OTBT SAM are shown in Fig. 6A and B respectively. For bare copper, the spectrum shows peaks at 489.5 and 405.9 cm^{-1}, which are assigned to copper oxides on the surface formed during the interval before polishing of the copper specimen and FTIR analysis [32]. The FTIR reflection absorption spectrum of 2-OTBT SAM covered copper shows the appearance of C—H stretching band at 2999 cm^{-1}, C=C stretching band at 1614 cm^{-1}, C=N stretching band at 1495 cm^{-1}, C—N stretching band at 1263 cm^{-1} and C—S stretching band at 757 cm^{-1}[33]. These peaks infer the presence of 2-OTBT on the copper surface. The lowering of C=N stretching band from 1600 cm^{-1} to 1495 cm^{-1} [34] and of C—N stretching band from 1276 cm^{-1} [33] to 1263 cm^{-1} infer the formation of complex between 2-OTBT SAM and copper surface through nitrogen atom. The vibration stretching band at 1754 cm^{-1} is attributed to the presence of ethyl acetate molecules in the SAM. This indicates that during the formation of 2-OTBT

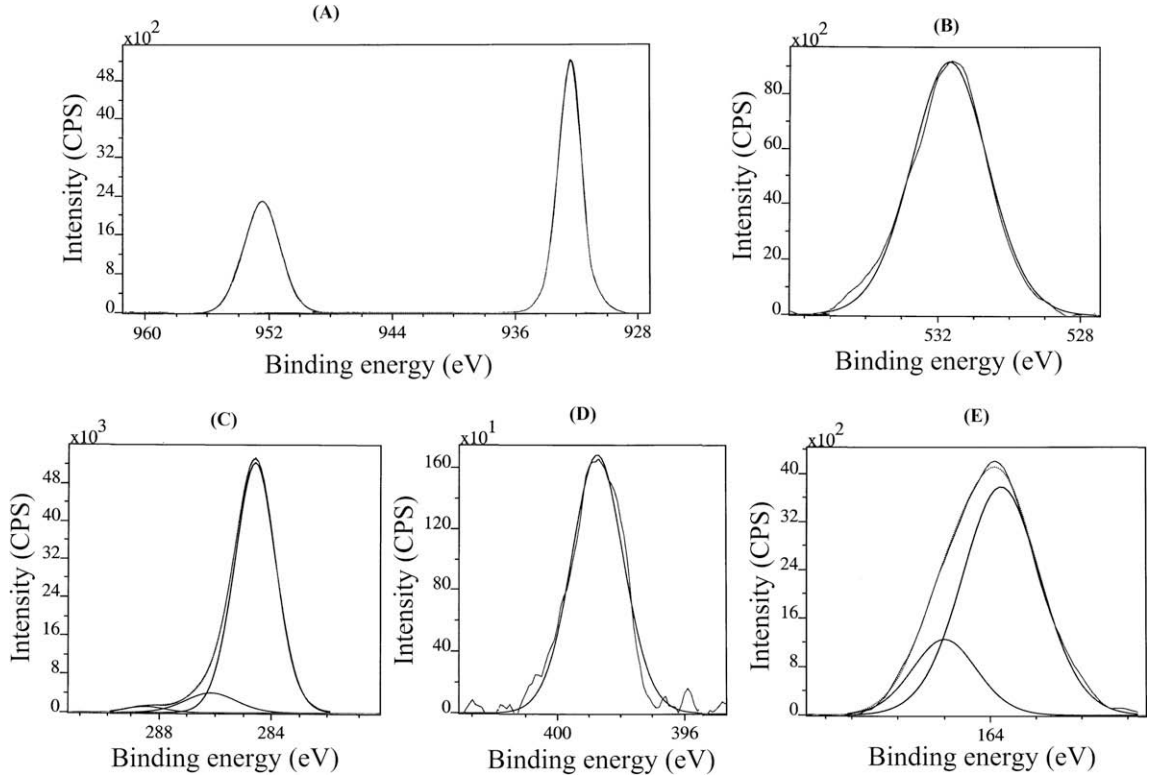

Fig. 5. (A–E) XPS deconvolution spectra of different elements present on the surface of the copper covered with 2-OTBT SAM (A – Cu 2p, B – O 1s, C – C 1s, D – N 1s, E – S 2p).

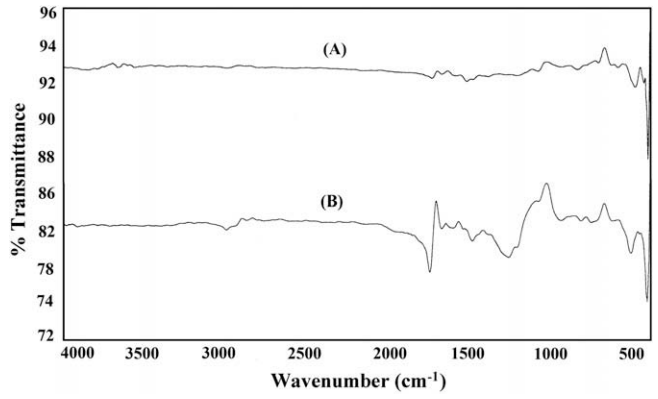

Fig. 6. (A) Reflection absorption FTIR spectrum of bare copper. (B) Reflection absorption FTIR spectrum of copper covered with 2-OTBT SAM.

SAM, some ethyl acetate molecules are also adsorbed on the copper surface. The vibration stretching bands at 414 and 515 cm^{-1} are due to the copper oxides formed due to initial oxidation of copper surface during formation of SAM.

3.2.4. AFM studies

AFM images for bare copper and copper covered with 2-OTBT SAM are shown in Fig. 7A and B respectively. Topographical changes of the copper surface in the absence and presence of 2-OTBT SAM are qualitatively characterized. AFM image of bare copper shows a homogenous film consisting of copper oxides, which are formed due to exposure of copper surface to the environment [35]. AFM image of SAM covered copper shows continuous small nodules, which cover the whole surface forming a protective layer. This layer entirely isolates the copper surface from the corrosive environment.

3.3. Corrosion protection of copper by 2-OTBT SAM

3.3.1. Electrochemical impedance studies in corrosive environments

Nyquist plots of bare copper and SAM covered copper electrodes are obtained in NaCl aqueous solutions after equilibration for 0.5 h, since the open-circuit potentials of the electrodes became steady within 0.5 h. Impedance parameters for the bare and SAM covered copper electrodes are obtained using two different equivalent circuit models [36], which are shown in Fig. 8A and B. The Nyquist plots of bare copper and SAM covered copper in NaCl solutions at different concentrations (0.02–0.20 M) at a constant immersion period of 0.5 h and at a constant temperature of 30 °C are shown in Fig. 9A and B, respectively, and the corresponding charge transfer resistance (R_{ct}), constant phase element (CPE) and n values are shown in Table 1. The small high-frequency semicircle, which is observed in the Nyquist plots for bare copper electrode in NaCl solutions is attributable to the single time constant of charge transfer resistance (R_{ct}) and the double-layer capacitance (C_{dl}) [37,38]. In the high frequency region, the electrode reaction is controlled by a charge transfer process and the diameter of the semicircle represents the charge transfer resistance (R_{ct}). Studies reported in the literature [39] showed that the diffusion process is controlled by diffusion of dissolved oxygen from the bulk solution to the electrode surface and the Warburg impedance, which is observed in the low frequency regions, is ascribed to diffusion of oxygen to the copper surface. The high frequency capacitive loop is so small that it is almost shielded by a straight line in the low frequency region. In NaCl solutions the corrosion reaction at bare copper surface consists of the anodic dissolution of copper and the cathodic reduction of the dissolved oxygen.

The Nyquist plots of 2-OTBT SAM covered copper electrodes are quite different from those of bare copper electrodes. For the SAM covered copper electrode, the Warburg impedance disappeared at low frequencies, indicating that the SAM is sufficiently densely packed to prevent the diffusion of oxygen to the copper substrate

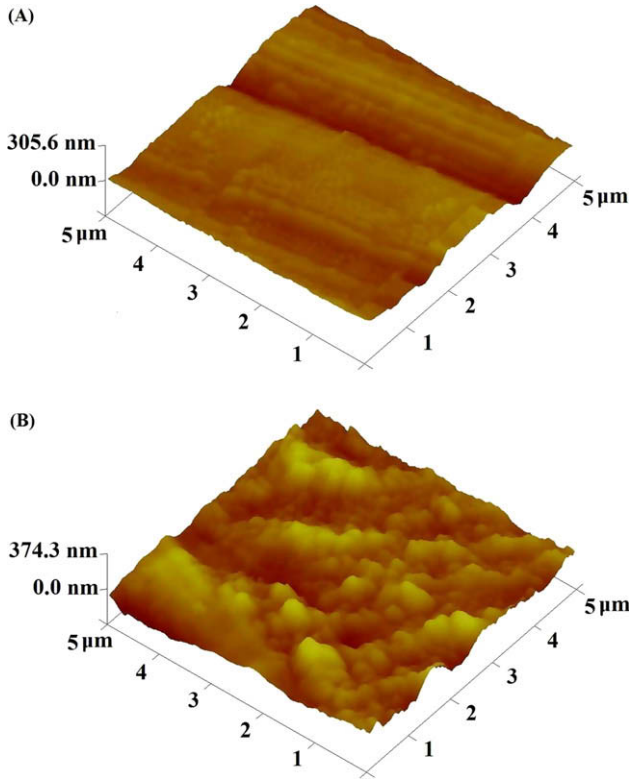

Fig. 7. (A) AFM image of bare copper. (B) AFM image of copper covered with 2-OTBT SAM.

and thus inhibit corrosion of copper. A large depressed semicircle is observed from high to low frequency regions in the Nyquist plots of SAM covered copper, indicating that the charge transfer resistance becomes dominant in the corrosion process due to the presence of protective SAM on the copper surface. In a practical electrode system, the impedance spectra are often depressed semicircles with their centres below the real axis. This phenomenon is known as the dispersing effect [40]. Due to the fact that the double-layer does not behave as an ideal capacitor in the presence of the dispersing effect, a constant phase element (CPE) is often used as a substitute for the capacitor in the equivalent circuit to fit the impedance behavior of the electrical double layer more accurately [40]. The CPE is a special element, whose value is a function of the angular frequency, ω, and whose phase is independent of the frequency. Its admittance and impedance are, respectively, expressed as

$$Y_{CPE} = Y_0(j\omega)^n \quad (1)$$

$$Z_{CPE} = 1/Y_0(j\omega)^{-n} \quad (2)$$

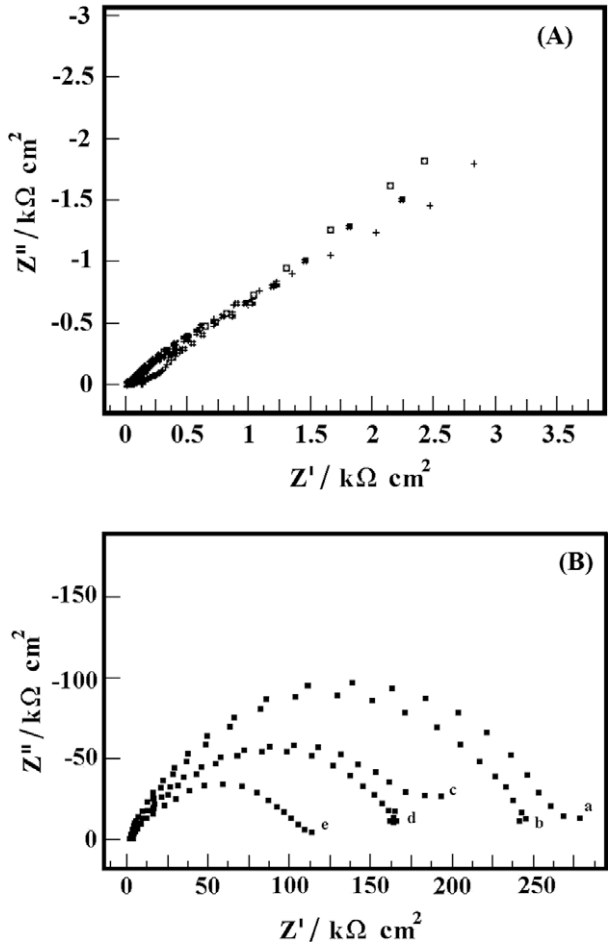

Fig. 9. (A) Nyquist plots of bare copper electrode in different concentrations of NaCl as corrosive environment. + – 0.02 M, ◘ – 0.05 M, # – 0.10 M, ■ – 0.15 M and $ – 0.20 M (Immersion period: 0.5 h, Temperature: 30 °C). (B) Nyquist plots of 2-OTBT SAM covered copper electrode in different concentrations of NaCl. a – 0.02 M, b – 0.05 M, c – 0.10 M, d – 0.15 M and e – 0.20 M (Immersion period: 0.5 h, temperature: 30 °C).

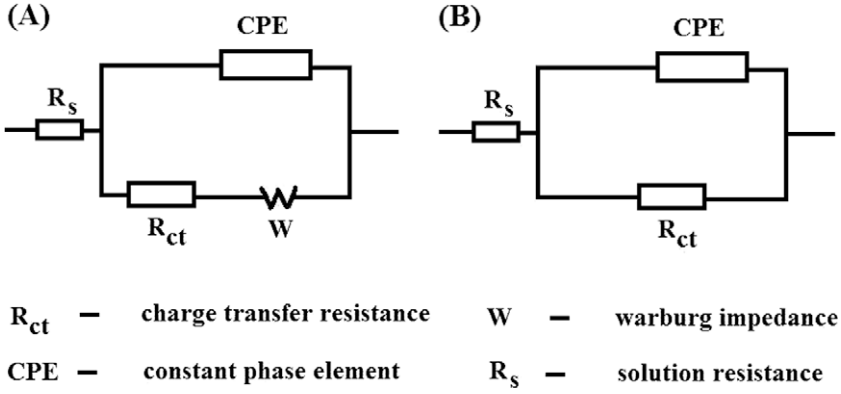

Fig. 8. (A) Equivalent circuit used in impedance measurements of bare copper electrode. (B) Equivalent circuit used in impedance measurements of copper electrode covered with 2-OTBT SAM.

Table 1
Impedance parameters of bare copper and copper covered with 2-OTBT SAM in NaCl environment at different concentrations (Immersion period: 0.5 h, temperature: 30 °C).

S.No.	Specimen	NaCl concentration (M)	Charge transfer resistance R_{ct} (kΩ cm^2)	Constant phase element CPE (μF/cm^2)	n	IE%
1	Bare copper	0.02	2.60	4.00	0.46	–
2	Copper with SAM	0.02	254.0	0.08	0.87	98.9
3	Bare copper	0.05	2.27	5.91	0.46	–
4	Copper with SAM	0.05	204.9	0.09	0.87	98.8
5	Bare copper	0.10	2.01	8.58	0.42	–
6	Copper with SAM	0.10	173.8	0.10	0.84	98.8
7	Bare copper	0.15	1.96	8.04	0.38	–
8	Copper with SAM	0.15	148.9	0.10	0.85	98.6
9	Bare copper	0.20	1.89	11.16	0.38	–
10	Copper with SAM	0.20	82.9	0.11	0.84	97.7

where Y_0 is the magnitude of the CPE, ω is the angular frequency and n is the exponential term of the CPE [40]. The n value is used to account for the roughness of the electrode. The lower the value of n, the rougher is the electrode surface. A smaller R_{ct} value corresponds to a higher corrosion rate. Nyquist plots for 2-OTBT SAM covered copper in 0.02 M NaCl showed a tendency for second time constant at lower frequencies as shown in Fig. 9B. This is due to the Faradaic reactions occurring on the surface [36]. The R_{ct} value for bare copper in 0.02 M NaCl is 2.60 kΩ cm^2, which increased enormously to 254.0 kΩ cm^2 for copper covered with 2-OTBT SAM in the same environment. The CPE value at the copper/0.02 M NaCl interface is found to decrease from 4.00 μF/cm^2 in the case of bare copper to a very small value such as 0.08 μF/cm^2 in the case of copper surface covered with 2-OTBT SAM. This is because the water molecules in the electrical double layer are replaced to a very large extent by the organic molecules having a very low dielectric constant [4]. In NaCl solutions the value of n has considerably increased in presence of SAM on copper surface. For example in 0.02 M NaCl environment, the value of n increased from 0.46 to 0.87 in the presence of SAM. These results indicate that the copper surface has become smoother due to formation of a non-porous and dense monolayer of 2-OTBT. The behavior of SAM tends to be an ideal capacitor when the value of n approaches unity gradually [41]. Inhibition efficiencies are found to be in the range of 98.9–97.7% in NaCl environment within the concentration range studied.

The Nyquist plots of bare copper and SAM covered copper in 0.02 M NaCl solutions at different immersion periods (0.5–24 h) and at a constant temperature of 30 °C are shown in Fig. 10A and B, respectively, and the corresponding charge transfer resistance (R_{ct}), constant phase element (CPE) and n values are shown in Table 2. With increase in immersion time, R_{ct} values decreased very slightly while CPE values increased very slightly and n values decreased very slightly after an exposure of SAM to the corrosive ions. Inhibition efficiencies are found to be in the range of 98.9–96.0% in 0.02 M NaCl environment within the immersion period range studied.

The Nyquist plots of bare copper and copper covered with 2-OTBT SAM in 0.02 M NaCl solutions at different temperatures (30–60 °C) and at a constant immersion period of 0.5 h are shown in Fig. 11A and B, respectively, and the corresponding charge transfer resistance (R_{ct}), constant phase element (CPE) and n values are shown in Table 3. The R_{ct} values are found to decrease for both bare copper and copper covered with SAM with increase in temperature. This observation is also supported by increase in CPE values and decrease in n values. Increase in temperature leads to an increase in corrosion rate in the absence and presence of corrosion inhibitors [42]. However, the inhibition efficiencies are found to be in the range of 98.9–92.1% in 0.02 M NaCl environment within the temperature range studied.

The studies of Nahir and Bowden [43] have shown that electrons can penetrate SAMs even though they are defect free. Moreover, the SAMs are found to contain molecule sized defects [44–47]. Zamborini and Crooks [44] proposed a corrosion reaction model for the electrode covered by SAMs with defects. In this model, the corrosive ions, such as halide ions, can permeate through SAMs through the defects and react with metal substrate, giving rise to the expansion of the defective sites and leading to further destruction of SAMs. Long hydrocarbon chains within the SAMs can partially heal the defects. 2-OTBT contains long hydrocarbon chain (octadecyl), two sulfur atoms and one nitrogen atom, which all together form a protective monolayer on the copper surface. The octadecyl chain heals the defects in the monolayer. The protective

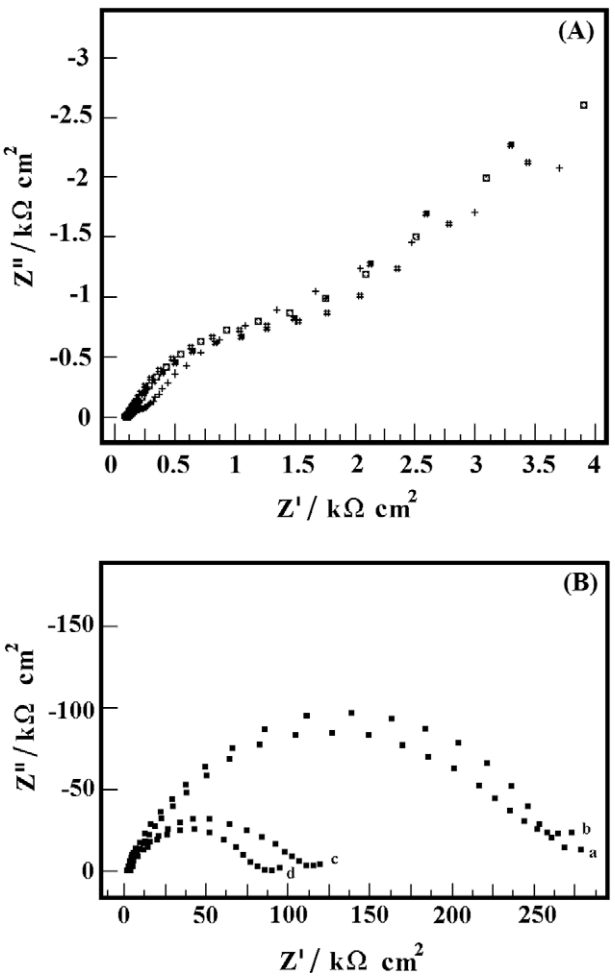

Fig. 10. (A) Nyquist plots of bare copper electrode in 0.02 M NaCl corrosive environment at different immersion periods. + – 0.5 h, ◘ – 6 h, # – 12 h and ■ – 24 h (Temperature: 30 °C). (B) Nyquist plots of 2-OTBT SAM covered copper electrode in 0.02 M NaCl at different immersion periods. a – 0.5 h, b – 6 h, c – 12 h and d – 24 h (Temperature: 30 °C).

Table 2
Impedance parameters of bare copper and copper covered with 2-OTBT SAM in 0.02 M NaCl environment at different immersion periods (Temperature: 30 °C).

S.No.	Specimen	Immersion time (h)	Charge transfer resistance R_{ct} (kΩ cm^2)	Constant phase element CPE (μF/cm^2)	n	IE%
1	Bare copper	0.5	2.60	4.00	0.46	–
2	Copper with SAM	0.5	254.0	0.08	0.87	98.9
3	Bare copper	6	2.58	6.81	0.46	–
4	Copper with SAM	6	224.6	0.10	0.84	98.8
5	Bare copper	12	2.46	7.30	0.45	–
6	Copper with SAM	12	99.3	0.23	0.75	97.5
7	Bare copper	24	2.42	8.93	0.45	–
8	Copper with SAM	24	60.5	0.34	0.71	96.0

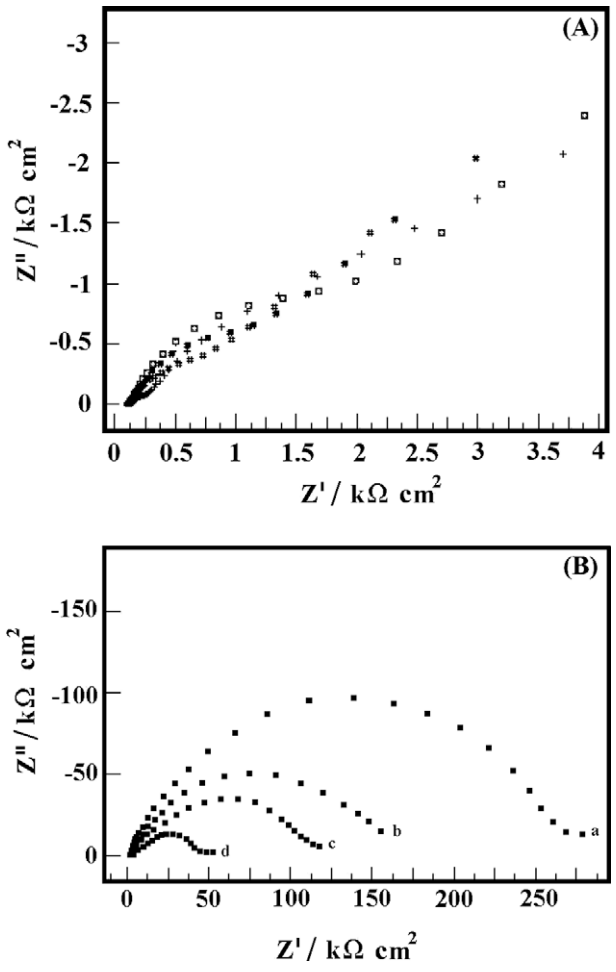

Fig. 11. (A) Nyquist plots of bare copper electrode in 0.02 M NaCl at different temperatures. + – 30 °C, ◘ – 40 °C, # – 50 °C and ■ – 60 °C (Immersion period: 0.5 h). (B) Nyquist plots of 2-OTBT SAM covered copper electrode in 0.02 M NaCl at different temperatures. a – 30 °C, b – 40 °C, c – 50 °C and d – 60 °C (Immersion period: 0.5 h).

film thus prevents the permeation of corrosive ions to the surface of copper and prevents corrosion.

Thus, all the observations in the impedance studies indicate that there is formation of a nonporous and highly protective SAM on copper surface, which effectively protects the metal surface from corrosion in aggressive NaCl environment, even at the immersion period of 24 h and temperatures up to 60 °C.

3.3.2. Results of studies using electrochemical quartz crystal nanobalance

Mass change of the SAM covered copper quartz crystal in 0.02 M NaCl environment at 30 °C is shown as a function of immersion time in Fig. 12. A very small negative mass change to an extent of only 0.20 μg/cm^2 even after 24 h immersion time demonstrates that the 2-OTBT monolayer formed on copper surface is stable even after 24 h of immersion period in 0.02 M NaCl solution.

3.3.3. Potentiodynamic polarization studies

Potentiodynamic polarization curves for bare copper and copper covered with 2-OTBT SAM have been obtained in NaCl solutions over a concentration range 0.02–0.20 M after an immersion period of 0.5 h and are shown in Fig. 13A and B respectively. The corrosion current densities (I_{corr}) have been determined from the

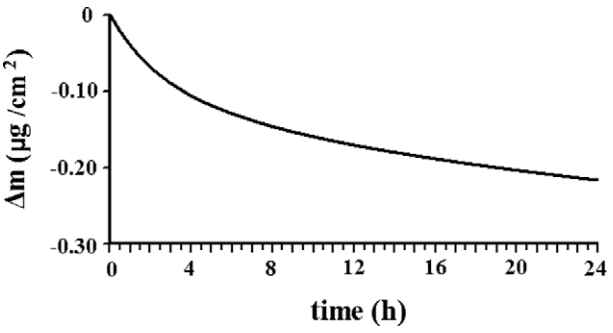

Fig. 12. Mass change vs. time curve of SAM of 2-OTBT on copper quartz crystal in corrosive environment, 0.02 M NaCl.

Table 3
Impedance parameters of bare copper and copper covered with 2-OTBT SAM in 0.02 M NaCl environment at different temperatures (Immersion period: 0.5 h).

S.No.	Specimen	Temperature (°C)	Charge transfer resistance R_{ct} (kΩ cm^2)	Constant phase element CPE (μF/cm^2)	n	IE%
1	Bare copper	30	2.60	4.00	0.46	–
2	Copper with SAM	30	254.0	0.08	0.87	98.9
3	Bare copper	40	2.50	5.79	0.45	–
4	Copper with SAM	40	141.0	0.11	0.79	98.2
5	Bare copper	50	2.44	7.71	0.45	–
6	Copper with SAM	50	86.2	0.13	0.80	97.1
7	Bare copper	60	2.40	8.84	0.41	–
8	Copper with SAM	60	30.5	0.45	0.69	92.1

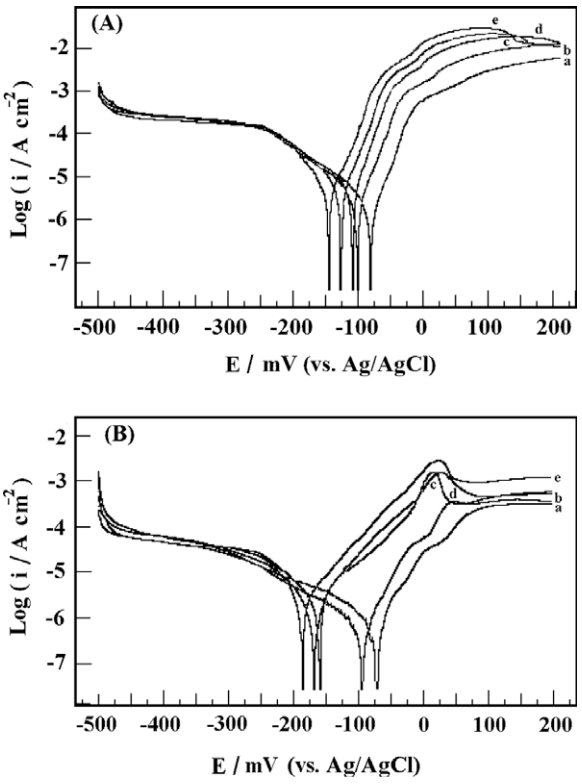

Fig. 13. (A) Potentiodynamic polarization curves of bare copper electrode in different concentrations of NaCl. a – 0.02 M, b – 0.05 M, c – 0.10 M, d – 0.15 M, e – 0.20 M (Immersion period: 0.5 h, Temperature: 30 °C). (B) Potentiodynamic polarization curves of 2-OTBT SAM covered copper electrode in different concentrations of NaCl. a – 0.02 M, b – 0.05 M c– 0.10 M, d – 0.15 M, e – 0.20 M (Immersion period: 0.5 h, temperature: 30 °C).

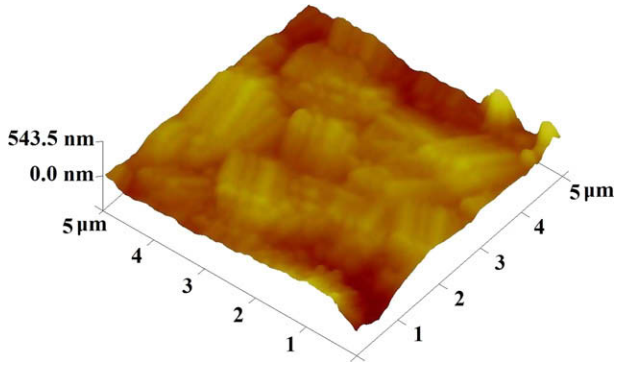

Fig. 14. AFM image of bare copper after 3 days immersion in 0.02 M NaCl solution.

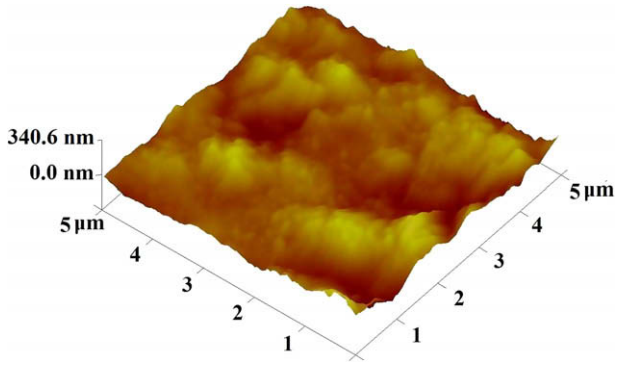

Fig. 15. AFM image of copper covered with 2-OTBT SAM after 3 days immersion in 0.02 M NaCl solution.

polarization curves by the tafel extrapolation method. SAM formed on the copper surface acts as a barrier to the diffusion of oxygen molecules from the solution to the copper surface, thereby resisting the transfer of oxygen to the cathodic sites of the copper surface. Compared with the bare copper, lower I_{corr} values are obtained for the SAM covered copper in NaCl solutions as shown in Table 4. With increase in NaCl concentration, I_{corr} values increased for bare copper to a much greater extent when compared to copper covered with SAM. The corrosion inhibition efficiencies of the SAM covered copper are in the range of 93.5–86.4%. These results are in good agreement with the efficiencies obtained from impedance studies. The corrosion potential (E_{corr}) of the copper electrode shifted towards more negative side after the deposition of SAM on copper surface. The cathodic tafel slope is shifted to a great extent in presence of the 2-OTBT SAM on the copper surface while the shift in anodic slope is very less. For example in 0.02 M NaCl, the cathodic tafel slope (b_c) is shifted from −433 to −183 mV/dec in presence of 2-OTBT SAM on the copper surface whereas the anodic slope is shifted from 80 to 60 mV/dec. Same is true at all the concentrations of the corrosive environment. It may be inferred that the 2-OTBT SAM on copper surface controls the cathodic reaction of the corrosion process and thus protects copper from corrosion.

3.3.4. Results of AFM studies

AFM image of bare copper is already shown in Fig. 7A. AFM image of bare copper after exposure to 0.02 M NaCl solution for 24 h is shown in Fig. 14. Topographical changes of the copper surface before and after immersion in 0.02 M NaCl are qualitatively char-

Table 4
Corrosion parameters obtained by potentiodynamic polarization studies of bare copper and copper covered with 2-OTBT SAM in NaCl environment at different concentrations (Immersion period: 0.5 h, temperature: 30 °C).

S.No.	Specimen	NaCl concentration (M)	E_{corr} (mV)	I_{corr} (µA/cm^2)	b_a (mV/decade)	b_c (mV/decade)	IE%
1	Bare copper	0.02	−83.4	11.9	80	−433	–
2	Copper with SAM	0.02	−73.8	0.77	60	−183	93.5
3	Bare copper	0.05	−99.6	14.1	64	−442	–
4	Copper with SAM	0.05	−97.7	1.08	65	−179	92.3
5	Bare copper	0.10	−108.6	16.0	52	−456	–
6	Copper with SAM	0.10	−158.2	1.59	63	−102	90.0
7	Bare copper	0.15	−128.7	17.2	56	−419	–
8	Copper with SAM	0.15	−165.4	2.14	88	−115	87.5
9	Bare copper	0.20	−147.0	19.6	60	−427	–
10	Copper with SAM	0.20	−186.6	2.65	80	−146	86.4

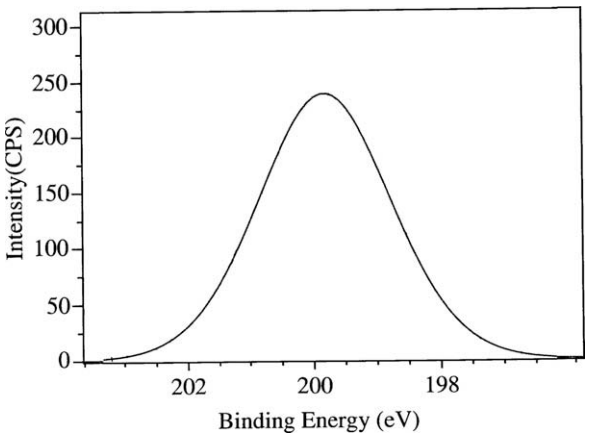

Fig. 16. XPS deconvolution spectrum of Cl 2p present on the surface of the bare copper after immersion in 0.02 M NaCl solution for a period of 3 days.

acterized. AFM image of bare copper shows a homogenous film consisting of Cu_2O, which is formed due to exposure of copper surface to the atmosphere [27]. AFM image for bare copper immersed in NaCl environment shows larger crystals, due to oxidation of copper surface in presence of chloride ions [48]. Copper activation is associated with the formation of two-dimensional salt layer of CuCl on the metal surface. In solutions containing low chloride concentration copper undergoes local activation (pitting), while in solutions with high chloride concentration, activation extends rapidly over the whole electrode surface [49].

AFM images of SAM covered copper before and after 24 h immersion in 0.02 M NaCl are shown in Figs. 7B and 15 respectively. AFM image of SAM covered copper (before immersion) shows continuous small nodules, which cover the whole surface forming a protective layer. This layer entirely isolates the copper surface from the corrosive environment. AFM image of copper covered with 2-OTBT SAM after immersion in NaCl environment also shows continuous and protective film with a very small change. From these AFM images it can be inferred that, 2-OTBT SAM is stable and protects the copper surface in aggressive environment such as 0.02 M NaCl even after 24 h immersion period.

3.3.5. Results of X-ray photoelectron spectroscopic studies

In the XPS survey spectrum of bare copper immersed in 0.02 M NaCl environment for 3 days, Cu $2p_{3/2}$, Cu $2p_{1/2}$ and O 1s peaks are detected, along with Cl 2p peak at 199.8 eV. The peaks due to Cu 2p and O 1s are similar to those shown in Fig. 4A and B. The peaks infer the formation of Cu_2O. The computer deconvolution spectrum for Cl 2p is shown in Fig. 16. This peak is due to formation of $CuCl_2$ on copper surface. The XPS spectrum of copper covered with 2-OTBT SAM after immersion in 0.02 M NaCl environment for 3 days shows peaks corresponding to Cu $2p_{3/2}$, Cu $2p_{1/2}$, O 1s, C 1s, N 1s and S 2p. The Cl 2p peak is absent. The computer deconvolution spectra for copper, oxygen, carbon, nitrogen and sulfur are shown in the Fig. 17. These spectra are compared with the corresponding spectra shown in Fig. 5A–E, for the 2-OTBT SAM modified copper substrate before immersion in the said corrosive environment. The intensities of Cu 2p peaks remained the same, while the intensities of C 1s, N 1s and S 2p peaks slightly decreased for 2-OTBT SAM covered copper after immersion in aq. 0.02 M NaCl environment. It is thus evident from the XPS spectra that the 2-OTBT SAM is stable even in the said corrosive environment and offers good protection to copper surface.

3.3.6. Results of weight-loss studies

Results of weight-loss studies for an immersion period of three days in 0.02 M NaCl environment, showed a corrosion rate of 0.0641 mm/yr for bare copper and only 0.0049 mm/yr for copper covered with 2-OTBT SAM. The relative standard error in corrosion rate determinations is of the order of 2% or less [50]. An inhibition

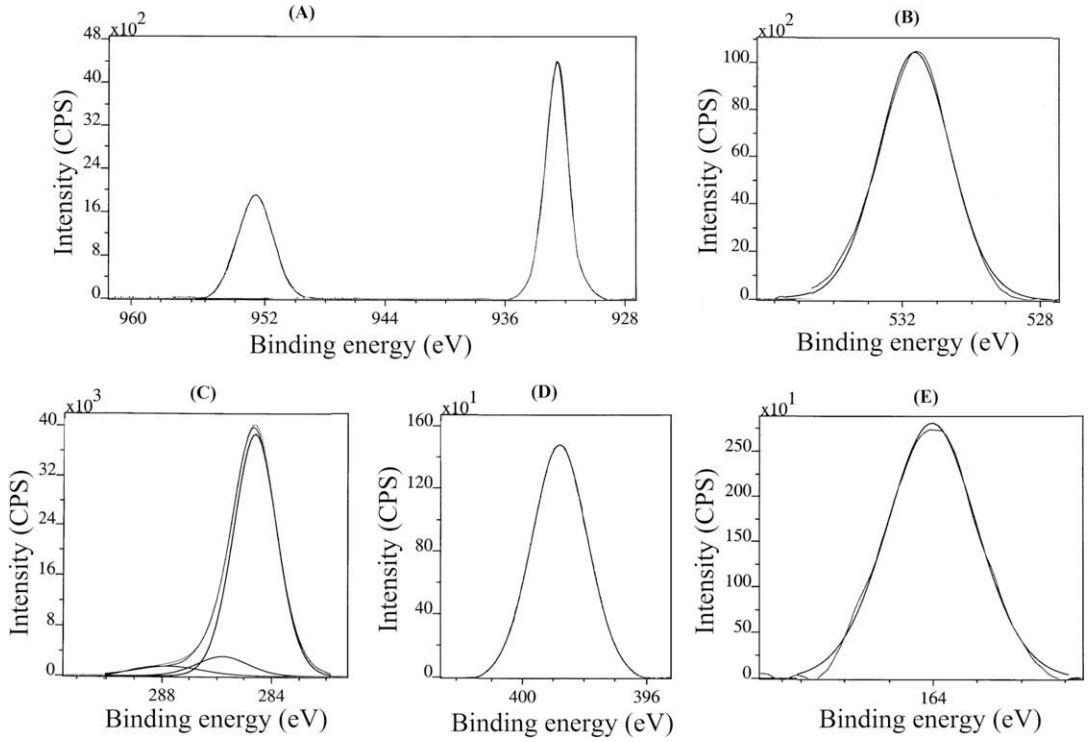

Fig. 17. (A–E) XPS deconvolution spectra of different elements present on the copper covered with 2-OTBT SAM after immersion in 0.02 M NaCl solution for a period of 3 days (A – Cu 2p, B – O 1s, C – C 1s, D – N 1s, E – S 2p).

Table 5
Quantum chemical parameters for 2-OTBT calculated by AM1 semi-empirical method.

E_{HOMO} (eV)	E_{LUMO} (eV)	ΔE (eV)	Net atomic charges									
			S(1)	C(2)	N(3)	C(4)	C(5)	C(6)	C(7)	C(8)	C(9)	Total ring charge
−9.593	−1.837	7.755	0.105	−0.110	−0.184	−0.023	−0.169	−0.135	−0.192	−0.182	−0.147	−1.041

efficiency of 92.3% is obtained from weight-loss studies. These results infer that the corrosion protection ability of the 2-OTBT SAM is quite good even after an immersion period of three days in the aggressive environment. The inhibition efficiency obtained from weight-loss studies is in good agreement with the values obtained from impedance studies and polarization studies though the immersion period is different in each of the methods.

3.3.7. Results of quantum chemical calculations

According to Fukui's frontier orbital approximation [51], interactions occur only between frontier molecular orbitals (MO), highest occupied molecular orbital (HOMO) and lowest unoccupied molecular orbital (LUMO) of both the reactants. It has been reported that the higher, the HOMO energy level of the inhibitor, the greater is the ease of offering electrons to the unoccupied d orbital of metallic copper and the greater the inhibition efficiency [52]. It is inferred that the more negative the atomic charges of the adsorbed centre, the more easily the atom donates its electrons to the unoccupied orbital of the metal [53]. It has also been reported that inhibitors can form coordination bonds between the unshared electron pair of the N atom, π electrons of aromatic ring and the unoccupied d electron orbital of the metal [54]. The larger the negative charge of the N atom, the better is the action as an electron donor. Table 5 shows the energy of the highest occupied molecular orbital (HOMO), energy of the lowest unoccupied molecular orbital (LUMO), the energy difference between LUMO and HOMO, the electron density for atoms in the ring and the total ring electron density for the 2-OTBT. The quantum chemical calculations [55–61] indicate that molecules with higher HOMO energy and lower energy gap between LUMO and HOMO provide higher corrosion inhibition efficiency. Thus, the greater inhibition efficiency of 2-OTBT for copper corrosion in NaCl solution can be attributed to the higher HOMO energy, lower energy gap between LUMO and HOMO and a very high negative total ring charge of the 2-OTBT molecule. The higher negative charge on N atom suggests the possibility of complex formation between Cu^+ ions and 2-OTBT through nitrogen.

The corrosion protection ability of 2-OTBT SAM was also tested in aq. HCl solutions (0.02–0.20 M) at various immersion periods and at various temperatures using all the methodologies as discussed above in the case of aq. NaCl as corrosive environment. It must be noted that the 2-OTBT SAM offers excellent corrosion protection of copper in aq. HCl environment also under the conditions specified. In view of the similarities between the results, the results of studies using aq. HCl as corrosive environment are not presented in the form of figures or tables.

3.4. Mechanistic aspects of corrosion protection by SAM

In the absence of SAM anodic dissolution of copper in chloride environment proceeds via a two-step oxidation process [23].

$$Cu + Cl^- \rightarrow CuCl + e^- \quad (3)$$

$$CuCl + Cl^- \rightarrow CuCl_2^- \quad (4)$$

The CuCl has poor adhesion and is unable to protect the copper surface, and transforms into the soluble cuprous chloride complex, $CuCl_2^-$ [62–64].

In neutral environment like NaCl, the presence of oxygen enhances the cathodic reaction due to oxygen reduction [65].

$$O_2 + 2H_2O + 4e^- \rightarrow 4OH^- \quad (5)$$

In the presence of 2-OTBT SAM, a plausible mechanism for corrosion protection of copper is shown in Fig. 18. The mechanism involves the formation of a non-porous, dense and protective monolayer of 2-OTBT on copper surface. The Cu^+ ions are formed due to initial corrosion during the formation of 2-OTBT SAM. Chelation occurs between the Cu^+ ions and the active sites (one nitrogen and two sulfur atoms) present in the 2-OTBT molecules. Long alkyl (octadecyl) chain present in the 2-OTBT molecule remains away from the copper surface. Due to the presence of Vander Waal forces between these neighboring alkyl chains, a hydrophobic, dense and defect-free monolayer is formed, which acts as a barrier between the copper surface and corrosive environment, thereby protecting the copper surface from corrosion. Tan et al. [25] reported the protective properties of self-assembled benzene thiols on copper. From the ellipsometric studies they reported that the molecular thicknesses of all the benzenethiol films on copper are less than 2 nm. They interpreted that the surface layer is restricted to a chemisorbed monolayer. If there is formation of multilayer through interaction via the benzene ring then the thickness should have been much higher. Some authors [66,67] have reported the film thickness of around 2 nm for the alkanethiol surface films. Here the intermolecular interaction between the alkyl chains is responsible for the formation of ordered monolayer but not a multilayer. Zhenlan Quan et al. [68] prepared self-assembled monolayers of schiff base on copper surface and immersed in a solution of 1-dodecanethiol to improve the corrosion protection of copper. They found that the thiol molecules subsequently adsorbed, were bonded directly on copper surface rather than physisorbed on the previous schiff base layer. They reported the formation of self-assembled monolayer but not of multilayer. Daiki Taneichi et al. [30] modified the self-assembled monolayers of 11-mercapto-1-undecanol using octyl and octadecyl isocyanates on copper surface and established their corrosion protection efficiency. They interpreted the inhibited films in terms of self-assembled monolayers. Chen Hao et al. [69] studied the corrosion protection ability of self-assembled monolayer of phytic acid on Cupronickel B30.

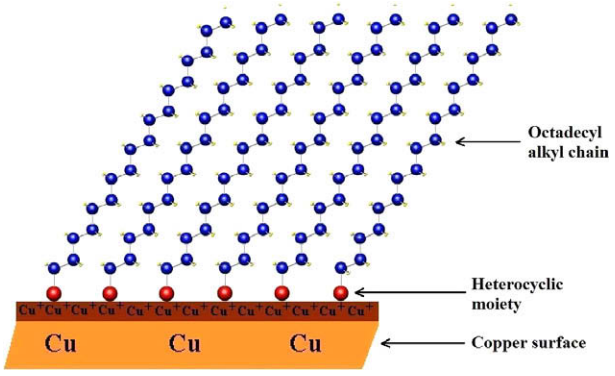

Fig. 18. Schematic illustration of mechanism of corrosion protection of copper by 2-OTBT SAM.

They showed that the adsorption mechanism of phytic acid is typical of chemisorption and follows langmuir's adsorption isotherm. They interpreted that the corrosion protection efficiency is because of the formation of self-assembled monolayer of phytic acid on the metal surface due to complexation between Cu^+ ions and phytic acid. Alagta et al. [70] studied the corrosion protection properties of self-assembled monolayers of hydroxamic acids with different alkyl lengths formed on copper surface and carbon steel. They demonstrated from the surface morphology studies by atomic force microscope [71] that there is formation of self-assembled monolayer only. In the light of the above results reported in the literature it is proposed that in the case of the present study of self-assembly of 2-(octadecylthio)benzothiazole, there is formation of a chemisorbed monolayer.

4. Conclusion

It is necessary to establish the optimum conditions for the formation of protective self-assembled monolayers of organic molecules on metal surfaces. The optimum conditions for the formation of protective SAM of 2-(octadecylthio)benzothiazole on copper surface are (i) etching of copper surface in 7 N nitric acid for 30 s (ii) ethyl acetate solvent (iii) 20 mM concentration of 2-OTBT and (iv) immersion time of 24 h. The SAM formed by 2-OTBT on copper surface offers excellent corrosion protection of copper in NaCl solution within the concentration range studied, i.e., up to 0.20 M at the ambient temperature, 30 °C. The 2-OTBT SAM offers good inhibition up to a temperature of 60 °C in 0.02 M NaCl solution. The inhibition efficiencies obtained from weight-loss studies, electrochemical impedance studies and polarization studies are in good agreement with each other. The nature of the protective monolayer formed on the copper surface plays a key role in the corrosion inhibition. The 2-OTBT molecules gets chemisorbed on copper surface and form a coordination complex with Cu^+ ions through nitrogen atom in the ring. The Vander Waal forces between long alkyl chains are responsible for the ordered monolayer.

Acknowledgements

One of the authors, Mr. Md. Yakub Iqbal is thankful to the National Institute of Technology Warangal, for providing the institute fellowship under the Technical Education Quality Improvement Programme of the Government of India.

References

[1] S.P. Murarka, Mater. Sci. Eng. R 19 (1997) 87.
[2] W.A. Lanford, P.J. Ding, Wei Wang, S. Hymes, S.P. Murarka, Mater. Chem. Phys. 41 (1995) 192.
[3] C.W. Tan, A.R. Daud, M.A. Yarmo, Appl. Surf. Sci. 191 (2002) 67.
[4] C.T. Wang, S.H. Chen, H.Y. Ma, L. Hua, N.X. Wang, J. Serb. Chem. Soc. 67 (10) (2002) 685.
[5] P.E. Laibinis, G.M. Whitesides, J. Am. Chem. Soc. 114 (1992) 9022.
[6] Y.Q. Feng, W.K. Teo, K.S. Siow, Z.Q. Gao, K.L. Tan, A.K. Hsieh, J. Electrochem. Soc. 144 (1997) 55.
[7] Y. Yamamoto, H. Nishihara, K. Aramaki, J. Electrochem. Soc. 140 (1993) 436.
[8] Z. Quan, X. Wu, S. Chen, S. Zhao, H. Ma, Corrosion 57 (2001) 195.
[9] Z. Quan, S. Chen, X. Cui, Y. Li, Corrosion 58 (2002) 248.
[10] R.L. Every, O.L. Riggs, Mater. Prot. 3 (1964) 46.
[11] V. Rajeswar Rao, V. Ravi Kumar, Indian J. Chem. B 41B (2002) 415.
[12] H. Tavakoli, T. Shahrabi, M.G. Hosseini, Mater. Chem. Phys. 109 (2008) 281.
[13] J.B. Brzoska, N. Shahidzadeh, F. Rondelez, Nature 360 (1992) 719.
[14] Miki Ishibashi, Miki Itoh, Hiroshi Nishihara, Kunitsugu Aramaki, Electrochim. Acta 41 (1996) 241.
[15] A. Shaban, E. Kalman, J. Telegdi, G. Palinkas, Gy. Dora, J. Appl. Phys. A 66 (1998) 545.
[16] N. Ohno, J. Uehara, K. Aramaki, J. Electrochem. Soc. 140 (1993) 2512.
[17] E. Szocs, Gy. Vastag, A. Shaban, G. Konczos, E. Kalman, J. Appl. Electrochem. 29 (1999) 1339.
[18] A. Shaban, E. Kalman, J. Bacskai, Proceedings of the 8th European Symposium on Corrosion Inhibitors, Ferrara, Italy, 1995, p. 951.
[19] D. Jope, J. Sell, H.W. Pickering, K.G. Weil, J. Electrochem. Soc. 142 (1995) 2170.
[20] Gy. Vastag, E. Szocs, A. Shaban, I. Bertoti, K. Popov Pergal, E. Kalman, Solid State Ionics 141–142 (2001) 87.
[21] J. Telegdi, A. Shaban, E. Kalman, Electrochim. Acta 45 (2000) 3639.
[22] G. Sauerbrey, Z. Phys. 155 (1959) 206.
[23] Myung M. Sung, Kiwhan Sung, Chang G. Kim, Sun S. Lee, Yunsoo Kim, J. Phys. Chem. B 104 (2000) 2273.
[24] J. Telegdi, T. Rigo, E. Kalman, Corros. Eng. Sci. Technol. 39 (2004) 65.
[25] Y.S. Tan, M.P. Srinivasan, S.O. Pehkonen, Simon Y.M. Chooi, Corros. Sci. 48 (2006) 840.
[26] X.R. Ye, X.Q. Xin, J.J. Zhu, Z.L. Xue, Appl. Surf. Sci. 135 (1998) 307.
[27] G. Petkova, E. Sokolova, S. Raicheva, P. Ivanov, J. Appl. Electrochem. 28 (1998) 1067.
[28] G.P. Cicileo, B.M. Rosales, F.E. Varela, J.R. Vilche, Corros. Sci. 41 (1999) 1359.
[29] Kamdem D. Pascal, Jun Zhang, Adnot Alain, Holzforschung 55 (2001) 16.
[30] Daiki Taneichi, Reiko Haneda, Kunitsugu Aramaki, Corros. Sci. 43 (2001) 1589.
[31] A.M. Beccaria, C. Bertolotto, Electrochim. Acta 42 (1997) 1361.
[32] G. Papadimitropoulos, N. Vourdas, V.Em. Vamvakas, D. Davazoglou, J. Phys: Conference series 10 (2005) 182.
[33] A. Lalitha, S. Ramesh, S. Rajeswari, Electrochim. Acta 51 (2005) 47.
[34] H. Baba, T. Kodama, K. Mori, H. Hirahara, Corros. Sci. 39 (1997) 555.
[35] Ch. Kleber, U. Hilfrich, M. Schreiner, Appl. Surf. Sci. 253 (2007) 3712.
[36] Guiyan Li, Houyi Ma, Yongli Jiao, Shenhao Chen, J. Serb. Chem. Soc. 69 (10) (2004) 791.
[37] O.E. Barcia, O.R. Mattos, N. Pebere, B. Tribollet, J. Electrochem. Soc. 140 (1993) 2825.
[38] Y. Feng, W.K. Teo, K.S. Siow, K.L. Tan, A.K. Hsieh, Corros. Sci. 38 (1996) 369.
[39] H. Ma, S. Chen, L. Niu, S. Zhao, S. Li, D. Li, J. Appl. Electrochem. 32 (2002) 65.
[40] X. Wu, H. Ma, S. Chen, Z. Xu, A. Sui, J. Electrochem. Soc. 146 (1999) 1847.
[41] H.Y. Ma, C. Yang, S.H. Chen, Y.L. Jiao, S.X. Huang, D.G. Li, J.L. Luo, Electrochim. Acta 48 (2003) 4277.
[42] A. Dafali, B. Hammouti, R. Touzani, S. Kertit, A. Ramdani, K. El Kacemi, Anti-Corros. Methods Mater. 49 (2) (2002) 96.
[43] T.M. Nahir, E.F. Bowden, Electrochim. Acta 39 (1994) 2347.
[44] F.P. Zamborini, R.M. Crooks, Langmuir 14 (1998) 3279.
[45] L. Sun, R.M. Crooks, Langmuir 9 (1993) 1951.
[46] O. Chailapakul, L. Sun, C. Xu, R.M. Crooks, J. Am. Chem. Soc. 115 (1993) 12459.
[47] X.M. Zhao, J.L. Wilbur, G.M. Whitesides, Langmuir 12 (1996) 3257.
[48] S. Kologo, M. Eyraud, L. Bonou, F. Vacandio, Y. Massiani, Electrochim. Acta 52 (2007) 3105.
[49] D. Starosvetsky, O. Khaselev, M. Auinat, Y. Ein-Eli, Electrochim. Acta 51 (2006) 5660.
[50] R.A. Freeman, D.C. Silverman, Corrosion 48 (1992) 463.
[51] H. Fujimoto, S. Kato, S. Yamabe, K. Fukui, J. Chem. Phys. 60 (1974) 572.
[52] C. Ogretir, B. Mihci, G. Bereket, J. Mol. Struct: Theochem. 488 (1999) 223.
[53] C.T. Wang, S.H. Chen, H.Y. Ma, C.S. Qi, J. Appl. Electrochem. 33 (2003) 179.
[54] D. Wang, S. Li, Y. Ying, M. Wang, H. Xiao, Z. Chen, Corros. Sci. 41 (1999) 1911.
[55] Y.I. Kuznetsov, I.A. Valuev, B. Electrochem. 3 (1987) 393.
[56] F.B. Growcock, W.W. Frenier, P.A. Andreozzi, Corrosion 45 (1989) 1007.
[57] V.S. Sastri, J.R. Perumareddi, Corrosion 50 (1994) 432.
[58] I. Lukovits, E. Kalman, G. Palinkas, Corrosion 51 (1995) 201.
[59] V.S. Sastri, J.R. Perumareddi, Corrosion 53 (1997) 617.
[60] I. Lukovits, E. Kalman, in: Proceedings of the 7th International symposium on Electrochemical methods in corrosion research, EMRC 2000, Budapest, Hungary, May 28, Paper No. 122, 2000, p. 1.
[61] I. Lukovits, K. Palfi, I. Bako, E. Kalman, Corrosion 53 (1997) 915.
[62] A. El Warraky, H.A. El Shayeb, E.M. Sherif, Anti-Corros. Methods Materi. 51 (2004) 52.
[63] E.M. Sherif, S.M. Park, J. Electrochem. Soc. 152 (2005) 428.
[64] C.W. Yan, H.C. Lin, C.N. Cao, Electrochim. Acta 45 (2000) 2815.
[65] H. Otmacic, E. Stupnisek-Lisac, Electrochim. Acta 48 (2003) 985.
[66] Yu-Wen Chang, Chijioke Ukiwe, Daniel Y. Kwok, Colloid. Surf. A 260 (2005) 255.
[67] T. Diem, W. Fabianowski, R. Jaccodine, R. Rodowski, Thin Solid Films 265 (1995) 71.
[68] Z. Quan, S. Chen, Y. Li, X. Cui, Corros. Sci. 44 (2002) 703.
[69] Chen Hao, Ren-He Yin, Zong-Yue Wan, Qun-Jie Xu, Guo-Ding Zhou, Corros. Sci. 50 (2008) 3527.
[70] A. Alagta, I. Felhosi, I. Bertoti, E. Kalman, Corros. Sci. 50 (2008) 1644.
[71] J. Telegdi, T. Rigo, E. Kalman, J. Electroanal. Chem. 582 (2005) 191.